In Vivo Specific Binding Characteristics and Pharmacokinetics of a 1,4-Dihydropyridine Calcium Channel Antagonist in the Senescent Mouse Brain

Shinya Uchida,[1,2] Shizuo Yamada,[1,4] Yoshiharu Deguchi,[1] Minoru Yamamoto,[3] and Ryohei Kimura[1]

Received April 3, 2000; accepted April 11, 2000

Purpose. To characterize the *in vivo* specific binding and pharmacokinetics of a 1,4-dihydropyridine (DHP) calcium channel antagonist, PN 200-110, in the senescent brain, using senescence-accelerated prone mice (SAMP8) and senescence-resistant mice (SAMR1).

Methods. Blood, brain, and heart samples were taken periodically from SAMR1 and SAMP8 following intravenous injection of (+)-[^{3}H]PN 200-110, and the concentration of (+)-[^{3}H]PN 200-110 in the plasma and tissues was determined. In addition, the *in vivo* specific binding of (+)-[^{3}H]PN 200-110 in the brains of SAMR1 and SAMP8 was measured periodically after intravenous injection of the radioligand.

Results. There was very little significant difference between SAMR1 and SAMP8 in terms of the half-life ($t_{1/2}$), total body clearance (CL_{tot}), steady-state volume of distribution (Vd_{ss}), and AUC for the plasma concentration of (+)-[^{3}H]PN 200-110 after intravenous injection of the radioligand. The brain concentration (AUC_{brain}) for (+)-[^{3}H]PN 200-110 and the brain/plasma AUC ratio (AUC_{brain}/AUC_{plasma}) were significantly lower in SAMP8 than in SAMR1, and the heart concentration (AUC_{heart}) and the heart/plasma AUC ratio (AUC_{heart}/AUC_{plasma}) were similar in both strains. Also, the brain/plasma unbound AUC ratio ($AUC_{brain}/AUC_{plasma\text{-}free}$) for (+)-[^{3}H]PN 200-110 was significantly lower in SAMP8 than in SAMR1. The *in vivo* specific binding ($AUC_{specific\ binding}$, maximal number of binding sites: B_{max}) of (+)-[^{3}H]PN 200-110 was significantly lower in brain particulate fractions of SAMP8 than SAMR1.

Conclusions. The concentration and *in vivo* specific binding of (+)-[^{3}H]PN 200-110 was significantly reduced in the senescent brain. The simultaneous analysis of the concentrations of centrally acting drugs and the *in vivo* specific binding in the brain in relation to their pharmacokinetics may be valuable in evaluating their CNS effects.

KEY WORDS: 1,4-dihydropyridine calcium channel antagonist; (+)-[^{3}H]PN 200-110; senescence-accelerated prone mouse; brain concentration; pharmacokinetics; *in vivo* receptor binding.

INTRODUCTION

The senescence-accelerated mouse (SAM) was developed by Takeda *et al.* (1) as a murine model of spontaneously accelerated aging. It consists of senescence-accelerated prone (SAMP) and senescence-resistant (SAMR) mice, and the latter exhibits normal aging characteristics. The P8 strain (SAMP8) was demonstrated to exhibit an age-related deterioration of learning and memory at an early age compared with a control strain, SAMR1 (2,3), which suggests that SAMP8 is useful as an experimental model for research on brain dysfunction during aging. Previous studies have also shown pathological and neurochemical alterations in the SAMP8 brain (4) and changes in receptors as well as in the concentration of various neurotransmitters (5,6). Recently, we have used *in vitro* radioligand binding studies to show that there was a significant reduction in the maximal number of binding sites (B_{max}) for (+)-[^{3}H]PN 200-110 in the brains of SAMP8 compared with SAMR1, and that chronic oral administration of nimodipine and nicardipine in SAMP8 increased significantly the B_{max} of (+)-[^{3}H]PN 200-110 binding in the cerebral cortex and hippocampus, with a significant improvement in learning deficit as assessed in the passive avoidance test (7). These observations are of interest in connection with the clinical effectiveness of nimodipine in treating senile dementia and age-related degenerative diseases (8).

Aging causes many physiological changes including reductions in hepatic blood flow, hepatic microsomal enzyme activity, glomerular filtration rate and lean body mass (9). These changes in the elderly lead to alterations in the pharmacokinetics (e.g., clearance and distribution) of calcium channel antagonists. In the case of isradipine, it has been reported that the plasma concentrations of this drug are higher in elderly people than in younger adults (10), and its volume of distribution in rats falls with age (11). However, in the SAMP8 strain, which exhibits spontaneously accelerated aging, the physiological changes governing the pharmacokinetics of such drugs were far from clear. In order to characterize the pharmacokinetics of a 1,4-dihydropyridine (DHP) calcium channel antagonist in SAMP8 as compared with SAMR1, we have measured the concentrations of (+)-[^{3}H]PN 200-110 in the plasma, brain and heart after intravenous injection, and subsequently, investigated the *in vivo* specific binding of (+)-[^{3}H]PN 200-110 in the brain of SAMP8 animals under more physiological conditions than is possible with *in vitro* specific binding. Our data demonstrated that the area under the curve for the brain concentration of (+)-[^{3}H]PN 200-110 in SAMP8 was smaller than that in SAMR1, while other pharmacokinetic parameters showed no difference between the two groups of animals. In addition, there was a significant reduction in the *in vivo* B_{max} of (+)-[^{3}H]PN 200-110 in the brains of SAMP8.

MATERIALS AND METHODS

Animals

This work was done in accordance with the *Principles of Laboratory Animal Care* (NIH publication #85-23, revised 1985). SAMP8 and SAMR1 were originally provided by Professor T. Takeda of the Department of Pathology, Chest Disease Research Institute, Kyoto University, and they were maintained

[1] Department of Biopharmacy, School of Pharmaceutical Sciences, University of Shizuoka, 52-1 Yada, Shizuoka 422-8526, Japan.
[2] Present address: Department of Hospital Pharmacy, Hamamatsu University School of Medicine, 3600 Handa-cho, Hamamatsu 431-3192, Japan.
[3] Clinical Pharmacology Research Lab, Yamanouchi Pharmaceutical Co., Ltd., Tokyo 174-8511, Japan.
[4] To whom correspondence should be addressed. (e-mail: yamada@-ys7.u-shizuoka-ken.ac.jp)

0724-8741/00/0700-0844$18.00/0

by brother-sister breeding in the Yamanouchi Pharmaceutical Research Laboratory at Tsukuba. Male SAMP8 and SAMR1, at 17 to 18 months of age, were used. Mice were housed under a 12-hr light-dark cycle and fed laboratory chow and water ad libitum.

Pharmacokinetic Studies

SAMP8 and SAMR1 received a single injection of 1.4 nmol/kg (120 kBq in 0.15 ml of saline) of (+)-[^{3}H]PN 200-110 in the tail vein. At 3, 5, 10 or 30 min after intravenous injection of (+)-[^{3}H]PN 200-110, blood was taken from the descending aorta under light anesthesia with diethylether and the brains (minus cerebellum and pons/medulla oblongata) and hearts were immediately removed and placed on ice. The tissues were homogenized in ice-cold 50 mM Tris-HCl buffer (pH 7.5) in final tissue concentrations of 20 mg/ml (brain) and 10 mg/ml (heart) using a Kinematica Polytron homogenizer. After the addition of scintillation fluids (AQUASOL II, DuPont-NEN Co. Ltd., Boston, MA), the radioactivity in plasma and aliquots of tissue homogenates was measured in a liquid scintillation counter. The remainder of the plasma, brain and heart of these mice were stored at −20°C to measure the concentration of unchanged (+)-[^{3}H]PN 200-110.

Determination of unchanged forms of (+)-[^{3}H]PN 200-110 was performed by a slight modification of the technique used to measure nilvadipine described previously by Tokuma *et al.* (12). Briefly, the brain and heart were homogenized in 1 ml of distilled water using a Polytron homogenizer. The plasma (0.05 ml) and aliquots (0.25 ml) of homogenates of the brain and heart were mixed with 0.1 volume ethanol, 1 volume 0.1 M borate buffer (pH 9.0) and 4 volumes benzene/hexane (1:1 v/v) mixture. The mixture was shaken for 5 min and centrifuged at about 10,000 × g for 10 min. The radioactivity in the organic phase was measured. In a preliminary experiment, the organic phase was spotted on TLC plates and developed with some mobile phases. There was only a peak of the same Rf value as the authentic sample, with a little peak of the major metabolites. The concentration of (+)-[^{3}H]PN 200-110 in the plasma, brain and heart represented that of unchanged drug. The data were expressed as Bq/ml/dose(MBq/kg) for plasma and Bq/g tissue (wet weight)/dose(MBq/kg) for brain and heart.

In vivo Specific Binding of(+)-[^{3}H]PN 200-110

In vivo measurement of specific (+)-[^{3}H]PN 200-110 binding in the mouse brain was performed by essentially the similar procedure as used in rat tissues (13,14). In the time course experiment, at 3, 5, 10 or 30 min after intravenous injection of (+)-[^{3}H]PN 200-110 (1.4 nmol/kg, 120 kBq) into the tail vein of SAMP8 and SAMR1 as described above, mice were sacrificed and the brains were dissected. In these experiments, at 30 min before intravenous injection of (+)-[^{3}H]PN 200-110, animals received vehicle and a "saturating dose" (40 mg/kg, i.p.) of nifedipine to determine total and nonspecific binding, respectively. Weighed samples of brain were homogenized in ice-cold 50 mM Tris HCl buffer to give a final tissue concentration of 20 mg/ml with a Kinematica Polytron homogenizer. The particulate-bound radioactivity was determined by rapid filtration of 1 ml of homogenate over Whatman GF/C filters which were then washed with 3 ml ice-cold buffer. The radioactivity in the filters was extracted by allowing them to stand at room temperature for 6 hr in scintillation fluid. The samples were counted by conventional scintillation spectrometry. The difference in the particulate-bound radioactivity in the brain homogenates between vehicle (total)- and nifedipine (nonspecific)-pretreated mice was defined as the *in vivo* specific (+)-[^{3}H]PN 200-110 binding. In a preliminary experiment, it was shown that there was no significant difference in the amount of *in vivo* specific (+)-[^{3}H]PN 200-110 binding following one and two washes with 3 ml ice-cold buffer of Whatman GF/C filters after filtration of brain homogenates. Thus, we considered that nonspecifically bound radioactivity could be removed by a single wash with 3 ml buffer under the present assay condition. The data were expressed as Bq/g tissue (wet weight)/dose(MBq/kg).

To construct saturation curves of (+)-[^{3}H]PN 200-110 binding to estimate the apparent dissociation constant (K_d) and maximal number of binding sites (B_{max}) in mouse brain, (+)-[^{3}H]PN 200-110 (120 kBq) and unlabeled (+)-PN 200-110 were combined in various ratios at total concentrations ranging from 27.2–330 nmol/kg in a volume of 0.15 ml and injected intravenously into the femoral vein to determine total binding. Nonspecific binding was determined as described above. A linear regression analysis of nonspecific binding at each dose was carried out. The resulting correlation coefficients ranged from 0.98 to 0.99. Specific binding was determined by subtracting the best-fit nonspecific vlaues from individual total binding values. Specific binding curves were fitted using the nonlinear regression analysis program MULTI (15) to the model (16) as follows: $\text{Bound} = B_{max} \cdot C_{plasma\text{-}free}/(K_d + C_{plasma\text{-}free})$. Values of B_{max} and K_d were expressed as pmol/g tissue and plasma-free concentration ($C_{plasma\text{-}free}$, nM), respectively.

Plasma Protein Binding

In vitro plasma protein binding of (+)-[^{3}H]PN 200-110 was determined by the equilibrium dialysis using a cellulose membrane (Sanplatec, Osaka, Japan). Briefly, mouse plasma containing (+)-[^{3}H]PN 200-110 was dialyzed with isotonic phosphate buffer (pH 7.4) at 37°C for 3 h. The radioactivity of (+)-[^{3}H]PN 200-110 in the dialysate fluid and plasma was measured as unbound ($C_{unbound}$) and total (C_{total}) (+)-[^{3}H]PN 200-110, respectively. The unbound fraction was calculated as $C_{unbound}/C_{total}$. $C_{plasma\text{-}free}$ was estimated as the product of the unbound fraction. The initial drug concentrations were 22.9, 45.8, 74.1, and 148 nM. Equilibrium was achieved by incubation for 3 h at 37°C. No signficant binding of (+)-[^{3}H]PN 200-110 to the dialysis membrane was observed.

Cerebral Blood Flow Rate

The measurement of the cerebral blood flow in mice with [^{14}C]iodoantipyrine was performed using essentially the procedure described by Jay *et al.* (17) and 60 kBq of [^{14}C]iodoantipyrine was infused into the femoral vein of SAMP8 and SAMR1 for 60 s at a rate of 0.1 ml/min. During this infusion time, blood samples were collected periodically (at 10-s intervals) from the femoral artery. Mice were sacrificed 60 sec after the infusion started, and the brains were dissected. The radioactivity in the brain and blood was determined.

Pharmacokinetic Analysis

Pharmacokinetic parameters were estimated by non-compartmental analysis from drug concentration-time profiles in plasma and tissues after intravenous injection of (+)-[^{3}H]PN 200-110 (18). The half-life ($t_{1/2}$) during the log-linear terminal phase was calculated from the elimination rate constant determined by linear regression analysis, and the area under the concentration *vs* time curve (AUC) was calculated by the trapezoidal rule for the observed values and subsequent extrapolation to infinity. The total body clearance (CL_{tot}) was calculated as dose/AUC, and the steady-state volume of distribution (Vd_{ss}) was determined by multiplying CL_{tot} by the mean residence time. The concentration of (+)-[^{3}H]PN 200-110 in brain (C_{br}) was determined by subtracting the amount remaining in vascular tissues from the total concentration (C_{tot}) using the following equation: $C_{br} = C_{tot} - V_p \times C_p$. C_p and V_p represent the plasma concentration of (+)-[^{3}H]PN 200-110 and the volume of distribution of [^{14}C]sucrose, a vascular marker that cannot penetrate the blood-brain barrier, respectively, at 5 min after intravenous injection in mice. The V_p was calculated by dividing the concentration of [^{14}C]sucrose in brain by that in plasma. In a preliminary experiment, the uptake of (+)-[^{3}H]PN 200-110 by blood cells was very small after intravenous injection. The partition coefficient of (+)-[^{3}H]PN 200-110 between tissue and plasma was calculated from the ratio of AUC in tissue (AUC_{brain} or AUC_{heart}) and AUC in plasma (AUC_{plasma}) (19,20). The area under the *in vivo* specific binding of (+)-[^{3}H]PN 200-110 vs time curve ($AUC_{specific\ binding}$) in brain was calculated as described above. All data are presented as mean ± S.D. Statistical analysis of all data was performed by Student's two-tailed t test. The level of statistical significance was accepted at $P < 0.05$.

Drugs

(+)-[^{3}H]PN 200-110 (3082 GBq/mmol), [^{14}C]iodoantipyrine (2.0 GBq/mmol) and [^{14}C]sucrose (17.6 GBq/mmol) were purchased from DuPont-NEN Co. Ltd. (Wilmington, DE). (+)-PN 200-110 was kindly donated by Sandoz Pharmaceuticals (Basle, Switzerland). All other chemicals were obtained from commercial sources.

RESULTS

Pharmacokinetics in Plasma, Brain, and Heart

Figure 1 shows the time course of the (+)-[^{3}H]PN 200-110 concentration in plasma, brain and heart of mice at 3, 5, 10 and 30 min after intravenous injection of the radioligand in SAMR1 and SAMP8. The volumes of distribution of [^{14}C]sucrose, used to estimate the concentration of (+)-[^{3}H]PN 200-110 in brain of SAMR1 and SAMP8 were 0.019 ± 0.002 (n = 4) and 0.019 ± 0.004 (n = 3) ml plasma/g tissue, respectively. The concentrations of (+)-[^{3}H]PN 200-110 in plasma, brain and heart attained maximum levels at 3 min, and, thereafter, the radioligand disappeared from plasma and both tissues in parallel. The concentration of (+)-[^{3}H]PN 200-110 in the brain of SAMR1 exceeded the plasma concentration, whereas that in SAMP8 was similar to the plasma level. The concentration of the radioligand in the heart of both SAMR1 and SAMP8 was much higher than the plasma level.

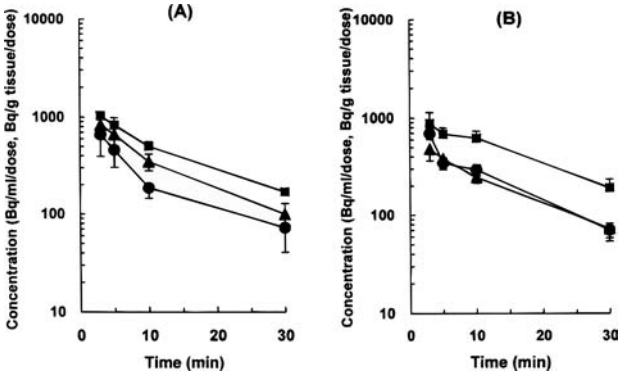

Fig. 1. Time courses of the (+)-[^{3}H]PN 200-110 concentration in plasma (●), brain (▲), and heart (■) of SAMR1 (A) and SAMP8 (B) after intravenous injection. (+)-[^{3}H]PN 200-110 (1.4 nmol/kg) was injected into the tail vein of mice, and at 3 to 30 min later, blood and brain were removed. The concentration of (+)-[^{3}H]PN 200-110 in brain was calculated by correcting for the brain plasma volume (V_p) which was determined by using [^{14}C]sucrose. The concentration was expressed as Bq/ml/dose (plasma) or Bq/g tissue/dose (brain, heart). Each point represents mean ± S.D. of three to eight mice.

The pharmacokinetic parameters of (+)-[^{3}H]PN 200-110 in plasma, brain and heart of SAMR1 and SAMP8 after intravenous injection were calculated. As shown in Table I, $t_{1/2}$, CL_{tot}, Vd_{ss} and AUC for the plasma concentration (AUC_{plasma}) of (+)-[^{3}H]PN 200-110 were similar in SAMR1 and SAMP8. Also, there was little significant difference between these animals as far as the $t_{1/2}$ for the concentration of (+)-[^{3}H]PN 200-110 in brain and heart was concerned. The AUC_{brain} for (+)-[^{3}H]PN 200-110, however, was significantly (34%) lower in SAMP8 than in SAMR1 (Table II). Similarly, there was a significant difference in AUC_{brain}/AUC_{plasma} for (+)-[^{3}H]PN 200-110 as shown by 0.88 ± 0.09 (SAMP8) and 1.50 ± 0.25 (SAMR1) ml/g tissue, respectively. On the other hand, AUC_{heart} and AUC_{heart}/AUC_{plasma} for (+)-[^{3}H]PN 200-110 in SAMP8 were similar to those in SAMR1.

The plasma protein binding for (+)-[^{3}H]PN 200-110 in SAMR1 and SAMP8 was measured. The unbound (free) fractions of (+)-[^{3}H]PN 200-110 in SAMR1 and SAMP8 were 10.1 ± 2.0 and 10.0 ± 2.5%, respectively. There was little significant difference in the unbound fraction among the initial drug concentrations (22.9–148 nM) in both animals. As shown in Table II, the $AUC_{brain}/AUC_{plasma\text{-}free}$ for (+)-[^{3}H]PN 200-110 in SAMP8 was significantly (41%) lower than that in SAMR1, while the $AUC_{heart}/AUC_{plasma\text{-}free}$ for (+)-[^{3}H]PN 200-110 in these mice was identical.

Table I. Pharmacokinetic Parameters Calculated from Concentrations of (+)-[^{3}H]PN 200-110 in Plasma After Intravenous Injection in SAMR1 and SAMP8[a]

Pharmacokinetic Parameters	SAMR1	SAMP8
$t_{1/2}$ (min)	9.49 ± 4.91	10.7 ± 2.6
CL_{tot} (ml/min/kg)	134 ± 19	119 ± 8
Vd_{ss} (ml/kg)	1810 ± 610	1680 ± 260
AUC (min · Bq/ml/dose)	7490 ± 1060	8410 ± 570

[a] Mean ± S.D. of 13 to 19 mice.

Table II. Pharmacokinetic Parameters and *In Vivo* Specific Binding of (+)-[^{3}H]PN 200-110 in Brain and Heart After Intravenous Injection in SAMR1 and SAMP8[a]

Pharmacokinetic parameters and *in vivo* specific binding	SAMR1	SAMP8
Pharmacokinetic parameters:		
(Brain)		
$t_{1/2}$ (min)	9.18 ± 3.21	10.4 ± 2.5
AUC_{brain} (min · Bq/g tissue/dose)	11200 ± 1100	7420 ± 580**
AUC_{brain}/AUC_{plasma} (ml/g tissue)	1.50 ± 0.25	0.88 ± 0.09*
$AUC_{brain}/AUC_{plasma\text{-}free}$ (ml/g tissue)	14.9 ± 2.5	8.80 ± 0.91*
(Heart)		
$t_{1/2}$ (min)	11.1 ± 3.1	13.1 ± 4.5
AUC_{heart} (min · Bq/g tissue/dose)	16200 ± 1100	17900 ± 2000
AUC_{heart}/AUC_{plasma} (ml/g tissue)	2.17 ± 0.34	2.13 ± 0.28
$AUC_{heart}/AUC_{plasma\text{-}free}$ (ml/g tissue)	21.5 ± 3.4	21.3 ± 2.8
In vivo specific binding		
$AUC_{specific\ binding}$ (min · Bq/ml/dose)	3750 ± 480	2670 ± 330*
$AUC_{specific\ binding}/AUC_{plasma\text{-}free}$ (ml/g)	4.97 ± 0.95	3.17 ± 0.44*

[a] Mean ± S.D. of 13 to 19 mice.
* Significantly different from the value of SAMR1, $P < 0.05$.
** Significantly different from the value of SAMR1, $P < 0.01$.

Measurement of *In Vivo* Specific Binding in Brain

The *in vivo* specific binding of (+)-[^{3}H]PN 200-110 in the particulate fraction of brains of SAMR1 and SAMP8 was measured at 3, 5, 10 and 30 min after intravenous injection of the radioligand (Fig. 2). The specific binding of (+)-[^{3}H]PN 200-110 in the SAMP8 brain was significantly lower (40%, $P < 0.05$) than that of SAMR1 at 5 min after intravenous injection. The $AUC_{specific\ binding}$ for *in vivo* specific binding was significantly (29%) lower in the brain of SAMP8 than SAMR1 (Table II). Also, the ratios of $AUC_{specific\ binding}$ to $AUC_{plasma\text{-}free}$ in SAMP8 and SAMR1 were 3.17 ± 0.44 and 4.97 ± 0.95 ml/g tissue, respectively, indicating a significant (36%) reduction in the senescent brain. As shown in Fig. 3, the concentrations of (+)-[^{3}H]PN 200-110 in the brains of SAMP8 and SAMR1 increased linearly with the increase in plasma free concentrations (1.42–21.6 nM) following the intravenous injection of various doses (27.2–330 nmol/kg) of the radioligand. Thus, the ratio of the concentration in the brain to the plasma free concentration at 5 min after intravenous injection of (+)-[^{3}H]PN 200-110 at doses of 27.2 to 330 nmol/kg was consistent both SAMR1 and SAMP8 (12.0 ± 1.3 and 8.19 ± 0.79 ml/g tissue, respectively, mean ± S.D., n = 12). In contrast, the *in vivo* specific binding of (+)-[^{3}H]PN 200-110 in brain of SAMP8 and SAMR1 appeared to be saturable with an increase in the plasma free concentration (1.42–21.6 nM), as shown in Fig. 4.

The *in vivo* maximal number of binding sites (B_{max}) for (+)-[^{3}H]PN 200-110 in brain of SAMP8 was significantly (47%) lower than that in SAMR1. On the other hand, there was little significant difference in the *in vivo* apparent dissociation constant (K_d) for (+)-[^{3}H]PN 200-110 between both strains (Table III).

There was no significant difference in AUC_{brain}/AUC_{plasma} for (+)-[^{3}H]PN 200-110 between vehicle (total)- and nifedipine (nonspecific)-pretreated mice (both SAMR1 and SAMP8), suggesting no significant effect of nifedipine pretreatment on the *in vivo* specific (+)-[^{3}H]PN 200-110 binding in the brains of SAMR1 and SAMP8.

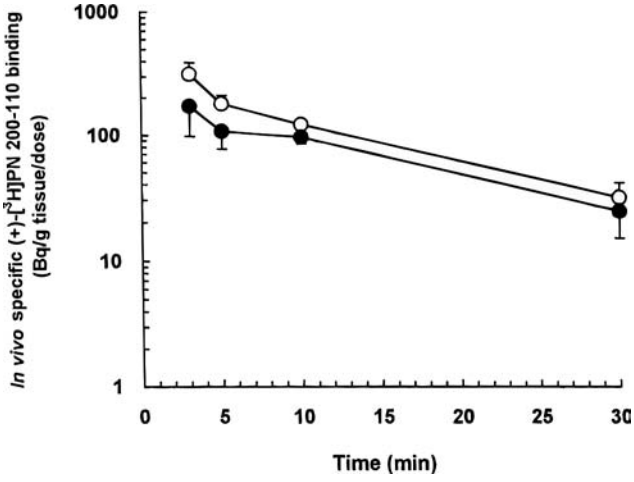

Fig. 2. Time course of *in vivo* specific binding of (+)-[^{3}H]PN 200-110 in brain of SAMR1 (◯) and SAMP8 (●) after intravenous injection. (+)-[^{3}H]PN 200-110 (1.4 nmol/kg) was injected into the tail vein of mice and 3 to 30 min later the specific binding was measured in particulate fractions of brain. Specific binding was expressed as Bq/g tissue/dose. Each point represents mean ± S.D. of three to eight mice.

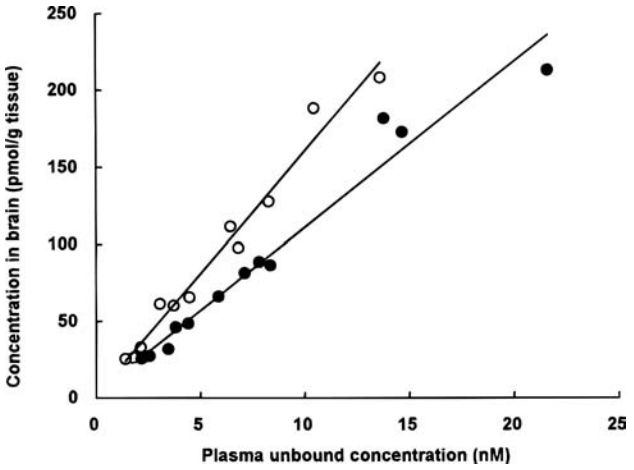

Fig. 3. Relationship between the plasma unbound concentration and brain concentration of SAMR1 (◯) and SAMP8 (●) after intravenous injection of (+)-[^{3}H]PN 200-110. (+)-[^{3}H]PN 200-110 (27.2–330 nmol/kg) was injected into the tail vein of mice and 5 min later the concentration of (+)-[^{3}H]PN 200-110 in the plasma and brain was measured. Each point represents the value from individual mice given (+)-[^{3}H]PN 200-110 intravenously. The points fit to a linear equation, SAMR1: $y = 16.0\ x + 1.20$, correlation coefficient $r = 0.988$ ($P < 0.01$), SAMP8: $y = 10.8\ x + 2.96$, $r = 0.981$ ($P < 0.01$), where y is the concentration in brain and x is the plasma unbound concentration.

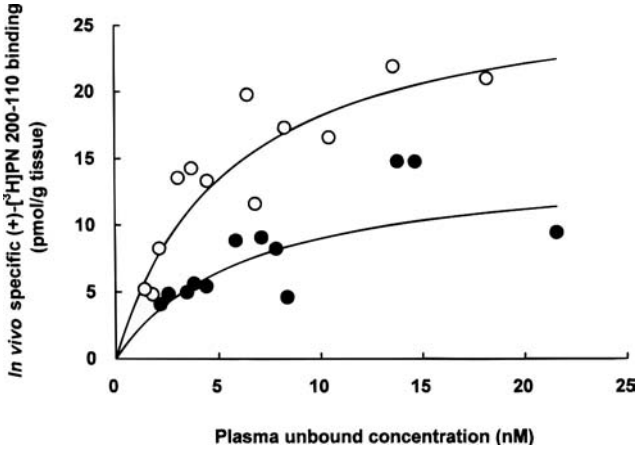

Fig. 4. *In vivo* specific binding of (+)-[^{3}H]PN 200-110 in brain of SAMR1 (◯) and SAMP8 (●) as a function of the increased plasma unbound concentration. (+)-[^{3}H]PN 200-110 (27.2–330 nmol/kg) was injected into the tail vein of mice and 5 min later the specific binding in particulate fractions of brain was measured. Each point represents the value from individual mice given (+)-[^{3}H]PN 200-110 intravenously. Solid lines were drawn by computer-generated nonlinear least-squares regression analysis.

Cerebral Blood Flow

The cerebral blood flow in SAMR1 and SAMP8 was measured by using [^{14}C]iodoantipyrine. There was little significant difference in cerebral blood flow (0.92 ± 0.01 vs 0.92 ± 0.11 ml/g brain/min, n = 4) between these strains.

DISCUSSION

The pharmacokinetics of (+)-[^{3}H]PN 200-110 in plasma, brain and heart of SAMR1 and SAMP8 was examined. The concentration of (+)-[^{3}H]PN 200-110 in the plasma, brain and heart of SAMR1 and SAMP8 following intravenous injection attained a maximum level at 3 min, and, thereafter, this radioligand disappeared from plasma and tissues in parallel. These data indicated that the distribution of (+)-[^{3}H]PN 200-110 to brain and heart was rapid and complete at 3 min after intravenous injection in these mice. There was little difference between SAMR1 and SAMP8 in terms of the pharmacokinetic parameters ($t_{1/2}$ CL_{tot}, Vd_{ss} and AUC) derived from the plasma concentrations of (+)-[^{3}H]PN 200-110.

It is well known that high lipophilicity is a prerequisite for effective transfer across the blood-brain barrier. Nimodipine is a highly lipophilic 1,4-DHP calcium channel antagonist, and has been shown to enter the brain freely (21). We have previously shown that (+)-[^{3}H]PN 200-110 as well as [^{3}H]nimodipine is extensively taken up into brain from plasma after intravenous injection in mice (22). In the present study, the brain concentration (AUC_{brain}) of (+)-[^{3}H]PN 200-110 after intravenous injection was significantly (34%) lower in SAMP8 than SAMR1. The ratio of AUC_{brain} or AUC_{heart} to $AUC_{plasma\text{-}free}$ of (+)-[^{3}H]PN 200-110 is considered to reflect the volume of distribution in the tissue. Although the ratio of AUC_{heart} to $AUC_{plasma\text{-}free}$ was identical between SAMR1 and SAMP8, the ratio of AUC_{brain} to $AUC_{plasma\text{-}free}$ for (+)-[^{3}H]PN 200-110 was significantly (41%) lower in SAMP8 than SAMR1. Also, the ratio of AUC_{brain} to AUC_{heart} for (+)-[^{3}H]PN 200-110 was lower in SAMP8 (0.41) than SAMR1 (0.69) (Table II). There was little significant difference in cerebral blood flow between SAMR1 and SAMP8. These data indicate that (+)-[^{3}H]PN 200-110 is taken up into the brain from the plasma to a lesser degree in SAMP8 than SAMR1, and that the concentration of the radioligand in the brain of SAMP8 is low, compared with SAMR1. Thus, it appears that the transport of (+)-[^{3}H]PN 200-110 through the microvascular walls in brain, which makes up the blood-brain barrier, is significantly restricted in SAMP8. This limitation might be partly due to the difference in the blood-brain barrier function between SAMP8 and SAMR1, as previously revealed in the brain transfer of blood-borne macromolecules in both strains (23). Currently, there is increasing evidence of the importance of efflux transport across the blood-brain barrier for drugs including 1,4-DHP calcium channel antagonists (24,25), since P-glycoprotein localizing at the luminal side of the brain capillaries has been shown to function as a drug efflux pump at the blood-brain barrier (26). It has been reported that the function of P-glycoprotein expressed in mouse lymphocytes is enhanced with aging (27). Accordingly, we cannot rule out the possibility that (+)-[^{3}H]PN 200-110 is pumped out of the SAMP8 brain to a significant degree via this functional protein in the blood-brain barrier.

In vivo occupation of 1,4-DHP calcium channel antagonist receptors in the brain of rats following intravenous injection of (+)-[^{3}H]PN 200-110 was previously reported (13,14). Our previous studies have shown that specific binding of (+)-[^{3}H]PN 200-110 in particulate fractions of rat brain after intravenous injection reflects predominantly *in vivo* binding to 1,4-DHP calcium channel antagonist receptors, because it was markedly inhibited by several 1,4-DHP agents (13,14). Similarly, a significant amount of *in vivo* specific binding was observed in particulate fractions of mouse brain following intravenous injection of (+)-[^{3}H]PN 200-110, [^{3}H]nifedipine and [^{3}H]nimodipine (22). In the present study, specific binding of (+)-[^{3}H]PN 200-110 was observed following intravenous injection of the radioligand both in SAMR1 and SAMP8, and it reached a maximum at 3 min after injection, then decreased with time. The time course of *in vivo* specific binding of (+)-[^{3}H]PN 200-110 followed that of the concentration in plasma and brain as described above. The *in vivo* specific binding of (+)-[^{3}H]PN 200-110 in the brains of SAMR1 and SAMP8 appeared to be saturable with an increase in plasma free concentration following different doses of the radioligand. It is unlikely that the saturability of *in vivo* (+)-[^{3}H]PN 200-110 binding is a result of the saturation of brain uptake of (+)-[^{3}H]PN 200-110, because the concentrations of (+)-[^{3}H]PN 200-110 in the brains of both SAMP8 and SAMR1 increased linearly with the

Table III. *In Vivo* Apparent Dissociation Constant (K_d) and Maximal Number of Binding Sites (B_{max}) for (+)-[^{3}H]PN 200-110 in Brains of SAMR1 and SAMP8[a]

	SAMR1	SAMP8
K_d (nM)	5.58 ± 1.90	6.48 ± 3.80
B_{max}(pmol/g brain)	28.3 ± 4.7	14.9 ± 4.2*

[a] Means ± S.D. of 12 mice.
* Significantly different from the value of SAMR1, $P < 0.05$.

increase in plasma free concentrations (Fig. 3). The estimated B_{max} for (+)-[^{3}H]PN 200-110 binding was significantly (47%) lower in brain particulate fractions of SAMP8 than in SAMR1. We have previously found, in an *in vitro* (+)-[^{3}H]PN 200-110 binding assay, that there is a consistently lowered density of 1,4-DHP calcium channel antagonist receptors in the cerebral cortex, hippocampus and corpus striatum of SAMP8 (7). Thus, the *in vitro* observation has been confirmed under physiological condition. It is conceivable that the reduction in brain concentration (AUC_{brain}) of (+)-[^{3}H]PN 200-110 after the intravenous injection in SAMP8, compared with SAMR1, is partly due to a reduced density of 1,4-DHP calcium channel antagonist receptors.

Although the mechanism responsible for the lowered density of 1,4-DHP calcium channel antagonist receptors in SAMP8 brain is at present uncertain, it is well known that neurotransmitter receptors can undergo compensatory regulation by modification of neuronal activity (28). Yamada *et al.* (7) have reported that the calcium content in the brain is markedly elevated in SAMP8 compared with SAMR1. Furthermore, age-related increases in brain calcium content have previously been shown (29). These results may indicate that the voltage-dependent calcium channel activity in brain is enhanced during the aging process. Thus, we postulate that an increase in the calcium channel activity in SAMP8 brain could lead to a compensatory down-regulation of 1,4-DHP calcium channel antagonist receptors. Down-regulation in response to the increased activity is a feature of calcium and potassium ion channels as well as neurotransmitter receptors (28). In SAMP8, therefore, a reduced 1,4-DHP calcium channel antagonist receptor density may lead to a change in brain calcium homeostasis and, subsequently, to brain dysfunction. This finding may have important clinical relevance, because the densities of 1,4-DHP calcium channel antagonist receptors have been found to be reduced in the cerebral cortex of patients with Alzheimer disease (30).

In conclusion, the present study has shown that the concentration and *in vivo* receptor binding of (+)-[^{3}H]PN 200-110 are significantly reduced in the brain of SAMP8 animals when compared with SAMR1. Our results show that the simultaneous analysis of the concentration and *in vivo* specific binding in the brain of centrally-acting drugs, in relation to their pharmacokinetics, may be a valuable aid in evaluating their CNS effects.

ACKNOWLEDGMENTS

This work was supported in part by Grant-in-Aid 07672470 for Scientific Research from the Ministry of Education, Science and Culture of Japan. The authors thank Miss T. Kusaka, Mr. H. Minaguchi and Miss K. Takahashi for their excellent technical assistance.

REFERENCES

1. T. Takeda, M. Hosokawa, S. Takeshita, M. Irino, K. Higuchi, T. Matsushita, Y. Tomita, K. Yasuhira, H. Hamamoto, K. Shimizu, M. Ishii, and T. Yamamuro. A new murine model of accelerated senescence. *Mech. Aging Dev.* **17**:183–194 (1981).
2. M. Miyamoto, Y. Kiyota, N. Yamazaki, A. Nagaoka, T. Matsuo, Y. Nagama, and T. Takeda. Age-related changes in learning and memory in the senescence-accelerated mouse (SAM). *Physiol. Behav.* **38**:399–406 (1986).
3. H. Yagi, S. Katoh, I. Akiguchi, and T. Takeda. Age-related deterioration of ability of acquisition in memory and learning in senescence accelerated mouse: SAM-P/8 as an animal model of disturbances in recent memory. *Brain Res.* **474**:86–93 (1988).
4. K. Higuchi, A. Matsumura, A. Honma, S. Takeshita, K. Hashimoto, M. Hosokawa, K. Yasuhira, and T. Takeda. Systemic senile amyloid in senescence-accelerated mouse. A unique fibril protein demonstrated in tissues from various organs by unlabeled immunoperoxidase method. *Lab. Invest.* **48**:231–240 (1983).
5. Y. Kitamura, X.-H. Zhao, T. Ohnuki, and Y. Nomura. Ligand-binding characteristics of [^{3}H]QNB, [^{3}H]prazosin, [^{3}H]rauwolscine, [^{3}H]TCP and [^{3}H]nitrendipine to cerebral cortical and hippocampal membranes of senescence accelerated mouse. *Neurosci. Lett.* **106**:334–338 (1989).
6. H. Kabuto, T. Yokoi, A. Mori, M. Murakami, and S. Sawada. Neurochemical changes related to ageing in the senescence-accelerated mouse brain and the effect of chronic administration of nimodipine. *Mech. Aging Dev.* **80**:1–9 (1995).
7. S. Yamada, S. Uchida, T. Ohkura, R. Kimura, M. Yamaguchi, M. Suzuki, and M. Yamamoto. Alterations in calcium antagonist receptors and calcium content in senescent brain and attenuation by nimodipine and nicardipine. *J. Pharmacol. Exp. Ther.* **277**:721–727 (1996).
8. P. K. Fischhof. Divergent neuroprotective effects of nimodipine in PDD and MID provide indirect evidence of disturbances in Ca^{2+} homeostasis in dementia. *Mech. Find. Exp. Clin. Pharmacol.* **15**:549–555 (1993).
9. J. G. Kelly and O'Malley. Calcium antagonists in the elderly. *Drugs Aging* **3**:400–407 (1993).
10. H. F. Schran, J. M. Jaffe, and L. M. Gonasum. Clinical pharmacokinetics of isradipine. *Am. J. Med.* **84(suppl. 3B)**:80–89 (1988).
11. F. L. S. Tse, J. M. Jaffe, A. E. Hassell, and H. F. Schran. Bioavailability of isradipine in young and old rats: effect of mode of administration. *J. Pharm. Pharmacol.* **41**:657–660 (1989).
12. Y. Tokuma, T. Fujiwara, and H. Noguchi. Absorption, distribution and excretion of nilvadipine, a new dihydropyridine calcium antagonist, in rats and dogs. *Xenobiotica* **17**:1341–1349 (1987).
13. S. Yamada, Y. Matsuoka, Y. Kato, R. Kimura, and O. Inagaki. A sustained occupancy *in vivo* of cardiovascular calcium antagonist receptors by mepirodipine and its relation to pharmacodynamic effect in spontaneously hypertensive rats. *J. Pharmacol. Exp. Ther.* **262**:589–594 (1992).
14. S. Uchida, S. Yamada, T. Ohkura, M. Heshikiri, A. Yoshimi, H. Shirahase, and R. Kimura. The receptor occupation and plasma concentration of NKY-722, a water-soluble dihydropyridine-type calcium antagonist, in spontaneously hypertensive rats. *Br. J. Pharmacol.* **114**:217–223 (1995).
15. K. Yamaoka, Y. Tanigawara, T. Nakagawa, and T. Uno. A pharmacokinetic analysis program (MULTI) for microcomputer. *J. Pharmacobiodyn.* **4**:879–885 (1981).
16. R. Weizman, A. Weizman, K. A. Kook, F. Vocci, S. I. Deutsh, and S. M. Paul. Repeated swim stress alters brain benzodizepine receptors measured *in vivo. J. Pharmacol. Exp. Ther.* **249**:701–707 (1989).
17. T. M. Jay, G. Lucignani, A. M. Crane, J. Jehle, and L. Sokoloff. Measurement of local cerebral blood flow with [^{14}C]iodoantipyrine in the mouse. *J. Cereb. Blood Flow Metab.* **8**:121–129 (1988).
18. M. Gibaldi and D. Perrier. *Pharmacokinetics (2nd Ed.)*, Marcel Dekker Inc., New York, Basel, 1982.
19. M. A. Gonzales, T. N. Tozer, and D. T. T. Chang. Nonlinear tissue disposition: salicylic acid in rat brain. *J. Pharm. Sci.* **64**:99–103 (1975).
20. M. A. Hedeya and R. J. Sawchuk. Effect of probenecid on the renal and nonrenal clearances of zidovudine and its distribution into cerebrospinal fluid in the rabbit. *J. Pharm Sci.* **78**:716–722 (1989).
21. D. S. Heffez, T. S. Nowak, and J. V. Passoneau. Nimodipine levels in gerbil brain following parenteral drug administration. *J. Neurosurg.* **63**:589–592 (1985).
22. S. Uchida, S. Yamada, K Nagai, Y. Deguchi, and R. Kimura. Brain pharmacokinetics and *in vivo* receptor binding of 1,4-dihydropyrine calcium channel antagonists. *Life Sci.* **61**:2083–2090 (1997).
23. M. Ueno, I. Akiguchi, H. Yagi, M. Takemura, T. Kitabayashi, J.

Kimura, M. Hosokawa, and T. Takeda. In T. Takeda (eds.), *Age-related changes in blood-brain barrier of the SAM brain. The SAM Model of Senescence*, Elsevier Science B. V., 1994, pp. 327–330.
24. M. M. Cornwell, I. Pastan, and M. M. Gottesman. Certain calcium channel blockers bind specifically to multidrug-resistant human KB carcinoma membrane vesicles and inhibit drug binding to P-glycoprotein. *J. Biol. Chem.* **262**:2166–2170 (1987).
25. I. Tamai and A. R. Safa. Azidopine noncompetitively interacts with vinblastine and cyclosporin A binding to P-glycoprotein in multidrug resistance cells. *J. Biol. Chem.* **266**:16796–16800 (1991).
26. A. Tsuji, T. Terasaki, Y. Takabataka, Y. Tenda, I. Tamai, T. Yamashima, S. Moritani, T. Tsuruo, and J. Yamashita. P-glycoprotein as the drug efflux pump in primary cultured bovine brain capillary endothelial cells. *Life Sci.* **51**:1427–1437 (1992).
27. S. Gupta. P-glycoprotein expression and regulation: age-related changes and potential effects on drug therapy. *Drugs Aging.* **7**:19–29 (1995).
28. M. D. Hollenberg. Examples of homospecific and heterospecific receptor regulation. *Trends Pharmacol. Sci.* **6**:242–245 (1985).
29. J. Cahn and M. G. Borzweix. Water, electrolytes contents of the brain and cerebral function in aged rats. *Monogr. Neural Sci.* **11**:85–92 (1984).
30. M. A. Piggott, J. M. Candy, and R. H. Perry. [^{3}H]Nitrendipine binding in temporal cortex in Alzheimer's and Huntington's diseases. *Brain Res.* **565**:42–47 (1991).